

SHORTENING THE TRAJECTORIES: IDENTITY-AWARE GAUSSIAN APPROXIMATION FOR EFFICIENT 3D MOLECULAR GENERATION

Jingxiang Qu¹, Wenhan Gao², Yi Liu^{2, 1}

¹ Department of Computer Science, Stony Brook University

² Department of Applied Mathematics & Statistics, Stony Brook University

ABSTRACT

Gaussian-based Probabilistic Generative Models (GPGMs) generate data by reversing a stochastic process that progressively corrupts samples with Gaussian noise. While these models have achieved state-of-the-art performance across diverse domains, their practical deployment remains constrained by the high computational cost of long generative trajectories, which often involve hundreds to thousands of steps during training and sampling. In this work, we introduce a theoretically grounded and empirically validated framework that improves generation efficiency without sacrificing training granularity or inference fidelity. Our key insight is that for certain data modalities, the noising process causes data to rapidly lose its identity and converge toward a Gaussian distribution. We analytically identify a characteristic step at which the data has acquired sufficient Gaussianity, and then replace the remaining generation trajectory with a closed-form Gaussian approximation. Unlike existing acceleration techniques that coarsening the trajectories by skipping steps, our method preserves the full resolution of learning dynamics while avoiding redundant stochastic perturbations between ‘Gaussian-like’ distributions. Empirical results across multiple data modalities demonstrate substantial improvements in both sample quality and computational efficiency.

1 INTRODUCTION

Generative models have achieved remarkable success in modeling complex data distributions across diverse modalities, including images, text, and molecular structures (Li et al., 2019; Austin et al., 2021; Zhang et al., 2023). One of the most commonly used pipelines is Gaussian-based Probabilistic Generative Models (GPGMs), which construct generative processes by learning to reverse a forward trajectory that incrementally corrupts data with Gaussian noise. While current GPGMs offer strong modeling flexibility and high sample quality, their practical deployment is often limited by the substantial computational cost associated with training and sampling over long generative trajectories. To mitigate this burden, recent studies have proposed trajectory coarsening techniques that skip redundant steps in the generation process (Song et al., 2020; Lu et al., 2022; Karras et al., 2022). However, such acceleration strategies typically compromise modeling granularity by omitting segments of the original sampling path, an intervention that may disrupt the continuity of the learned dynamics and degrade the model fidelity. Furthermore, most existing methods fail to reduce training steps without sacrificing the granularity necessary for effective learning.

In this work, we propose a novel method that improves the efficiency of Gaussian-based generative processes. Rather than coarsening the learned trajectories by skipping steps, our method identifies a characteristic time step T^* at which the input data distribution has effectively lost its specific identity while gaining sufficient Gaussianity. *Based on this point, the generation trajectory can be analytically truncated, and the final distribution can be approximated by a tractable Gaussian reference distribution, as shown in Fig. 1.* This permits the reuse of the original noise schedule with fine learning granularity while avoiding redundant transport among ‘Gaussian-like’ distributions. We empirically validate our method across generative tasks involving different data modalities, demonstrating significant improvements in both sampling and training efficiency with high-quality generation.

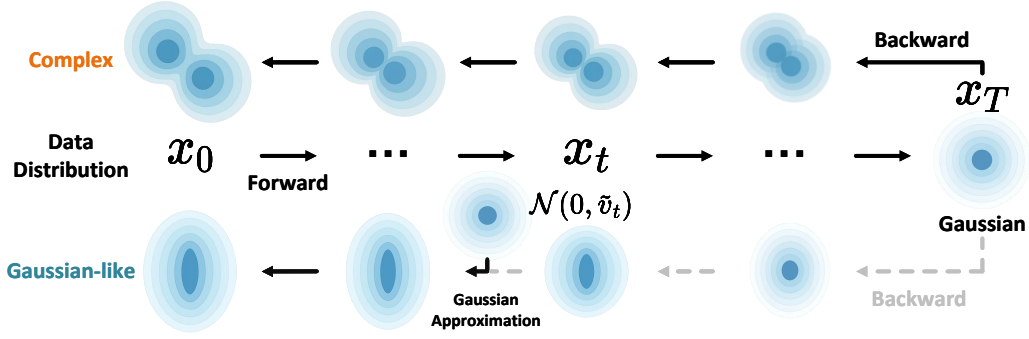


Figure 1: The flowchart of the Gaussian approximation. For a zero-meaned, Gaussian-like data distribution, we approximate the distribution of \mathbf{x}_t with a reference Gaussian $\mathcal{N}(0, \tilde{v}_t)$ once it becomes sufficiently close to Gaussian at timestep t . In this case, the length of the generative trajectory can be reduced from T steps to t steps.

2 PRELIMINARIES

2.1 GAUSSIAN-BASED PROBABILISTIC GENERATIVE MODELS

GPGMs construct complex data distributions by learning to reverse a reference stochastic process that progressively corrupts clean data with Gaussian noise. Given a data sample \mathbf{x}_0 drawn from the target distribution $p_{\text{data}}(\mathbf{x})$, we define a forward (noising) process that maps \mathbf{x}_0 to a sequence of latent states $\{\mathbf{x}_t\}_{t=1}^T$. A commonly used instantiation of this noising process is a time-indexed Gaussian perturbation:

$$q(\mathbf{x}_t | \mathbf{x}_0) = \mathcal{N}(\mathbf{x}_t | \sqrt{\bar{\alpha}_t} \mathbf{x}_0, \bar{\sigma}_t^2 \mathbf{I}), \quad (1)$$

where $\bar{\alpha}_t \in [0, 1]$ controls the decay of the signal power over time. Typically, $\bar{\alpha}_t$ is defined as $\bar{\alpha}_t = \prod_{s=1}^t \alpha_s$, with $\alpha_t \in (0, 1)$ monotonically decreasing such that $\bar{\alpha}_0 \approx 1$ and $\bar{\alpha}_T \approx 0$, ensuring that \mathbf{x}_T approaches a tractable reference distribution, often taken to be $\mathcal{N}(\mathbf{0}, \bar{\sigma}_T^2 \mathbf{I})$.

In the case of variance-preserving (VP) forward processes, defined by $\bar{\sigma}_t = \sqrt{1 - \bar{\alpha}_t}$, the forward process admits the following Markov factorization:

$$q(\mathbf{x}_{1:T} | \mathbf{x}_0) = \prod_{t=1}^T q(\mathbf{x}_t | \mathbf{x}_{t-1}) = \prod_{t=1}^T \mathcal{N}(\mathbf{x}_t | \alpha_{t|t-1} \mathbf{x}_{t-1}, \sigma_{t|t-1}^2 \mathbf{I}), \quad (2)$$

where $\alpha_{t|t-1} = \bar{\alpha}_t / \bar{\alpha}_{t-1}$ and $\sigma_{t|t-1}^2 = 1 - \alpha_{t|t-1}^2$. The VP forward process is the most commonly used formulation in the design of GPGMs. Unless otherwise specified, we adopt the VP noising schedule throughout this work.

The reverse (denoising) process, which models $p(\mathbf{x}_{t-1} | \mathbf{x}_t)$, admits a closed-form expression under the Gaussian assumption:

$$q(\mathbf{x}_{t-1} | \mathbf{x}_t, \mathbf{x}_0) = \mathcal{N}(\mathbf{x}_{t-1} | \boldsymbol{\mu}_t(\mathbf{x}_t, \mathbf{x}_0), \tilde{\sigma}_t^2 \mathbf{I}), \quad (3)$$

where

$$\boldsymbol{\mu}_t(\mathbf{x}_t, \mathbf{x}_0) = \frac{\sqrt{\bar{\alpha}_{t-1}}(1 - \bar{\alpha}_t)}{1 - \bar{\alpha}_{t-1}} \mathbf{x}_0 + \frac{\sqrt{\bar{\alpha}_t}(\bar{\alpha}_{t-1} - \bar{\alpha}_t)}{1 - \bar{\alpha}_{t-1}} \mathbf{x}_t, \quad \tilde{\sigma}_t^2 = \frac{(1 - \bar{\alpha}_t)(1 - \bar{\alpha}_{t-1})}{1 - \bar{\alpha}_{t-1}}.$$

This Gaussian formulation facilitates a tractable variational objective and enables efficient sampling algorithms that are central to GPGMs.

Learning the Reverse Process A key feature of GPGMs is that the reverse-time generative process is constructed to approximate the true posterior $q(\mathbf{x}_{t-1} | \mathbf{x}_t, \mathbf{x}_0)$. Since the original sample \mathbf{x}_0 is unavailable during generation, it is replaced by a neural estimate $\hat{\mathbf{x}}_0 = \phi(\mathbf{x}_t, t)$ inferred from the current noisy observation. The generative transition distribution is then defined as:

$$p(\mathbf{x}_{t-1} | \mathbf{x}_t) = \mathcal{N}(\mathbf{x}_{t-1} | \boldsymbol{\mu}_t(\mathbf{x}_t, \hat{\mathbf{x}}_0), \tilde{\sigma}_t^2 \mathbf{I}), \quad (4)$$

where the mean and variance retain the form of the true posterior, with \mathbf{x}_0 replaced by its approximation $\hat{\mathbf{x}}_0$. Given this generative model, we can derive a variational lower bound on the marginal log-likelihood:

$$\log p(\mathbf{x}_0) \geq \mathcal{L}_0 + \mathcal{L}_{\text{base}} + \sum_{t=1}^T \mathcal{L}_t, \quad (5)$$

where $\mathcal{L}_0 = \log p(\mathbf{x}_0 | \mathbf{x}_1)$ is the terminal reconstruction term, $\mathcal{L}_{\text{base}} = -\text{KL}(q(\mathbf{x}_T | \mathbf{x}_0) \| p(\mathbf{x}_T))$ regularizes the marginal at the final time step, and

$$\mathcal{L}_t = -\text{KL}(q(\mathbf{x}_{t-1} | \mathbf{x}_0, \mathbf{x}_t) \| p(\mathbf{x}_{t-1} | \mathbf{x}_t)), \quad \text{for } t = 1, \dots, T. \quad (6)$$

In practice, the base KL term $\mathcal{L}_{\text{base}}$ becomes negligible when $\alpha_T \approx 0$, and the data term \mathcal{L}_0 is often near zero for discrete \mathbf{x}_0 when $\alpha_0 \approx 1$. Meanwhile, Ho et al. (2020) found it more stable to parameterize ϕ as a noise predictor: rather than outputting $\hat{\mathbf{x}}_0$ directly, the network predicts the noise vector $\hat{\epsilon}$ such that $\mathbf{x}_t \approx \alpha_t \mathbf{x}_0 + \sigma_t \epsilon$. In this case, $\hat{\mathbf{x}}_0$ can be recovered via $\hat{\mathbf{x}}_0 = \frac{1}{\alpha_t} (\mathbf{x}_t - \sigma_t \hat{\epsilon})$. This formulation leads to a simplified training objective, where each KL term \mathcal{L}_t reduces to a weighted denoising score-matching loss:

$$\mathcal{L}_t = \mathbb{E}_{\epsilon \sim \mathcal{N}(\mathbf{0}, \mathbf{I})} \left[\frac{1}{2} w_t \|\epsilon - \hat{\epsilon}\|^2 \right], \quad (7)$$

where w_t is a scalar weight derived from the noise schedule. This structure naturally extends to various GPGM frameworks, such as diffusion models (Ho et al., 2020) and flow-matching models (Lipman et al., 2022), both of which aim to approximate the conditional dynamics of the reverse process via supervised regression on progressively removed noise.

2.2 ZERO-MEAN INVARIANCE

A data modality is *zero-mean invariant* if centering each sample by subtracting its empirical mean preserves all the information necessary for downstream modeling. Formally, let $x \in \mathbb{R}^d$ denote a data sample, and define its centered version as:

$$\tilde{x} = x - \frac{1}{d} \sum_{i=1}^d x_i \cdot \mathbf{1}_d, \quad (8)$$

where $\mathbf{1}_d \in \mathbb{R}^d$ is the vector of all 1-s. A data modality is said to satisfy zero-mean invariance if, for all x in the support of the data distribution $p(x)$, the transformation $x \mapsto \tilde{x}$ retains the semantic or structural identity of the original input.

This property is common in domains where only internal relationships among dimensions carry information, while global offsets are irrelevant or redundant. Typical examples include any representations defined up to an affine baseline or possessing a shift-symmetric structure, such as configurations invariant to global alignment, label encodings invariant to additive bias, or features embedded in contrastive spaces. Zero-mean invariance permits generative models to operate in a reduced subspace orthogonal to the mean direction, eliminating redundant degrees of freedom. In geometric learning, zero-mean invariance is widely employed due to the translational invariance of geometric data representation (Hoogetboom et al., 2022; Hong et al., 2025; Xu et al., 2023).

3 SHORTENING GENERATIVE TRAJECTORIES

Building on the theoretical preliminaries, we now introduce our framework for shortening the generative trajectory in GPGMs via truncation. Rather than executing the full generation trajectories, we identify a characteristic timestep T^* at which the data effectively loses its identity and exhibits sufficient Gaussianness. This enables an analytic truncation, whereby the remaining trajectory is replaced with a direct Gaussian approximation. It significantly improves computational efficiency without compromising generative fidelity.

3.1 GAUSSIAN APPROXIMATION

Gaussian approximations (GA) are commonly employed in statistics to represent intractable conditional or marginal distributions (Berry, 1941; Deng & Zhang, 2020; Chernozhukov et al., 2013). This modeling choice facilitates closed-form expressions for critical quantities, including transition densities, posterior distributions, and variational bounds, which are essential for both optimization and sampling procedures. In GPGMs, the forward process can be interpreted as progressively pushing the data toward a Gaussian distribution. As illustrated in equation 1, the marginal and transition densities of the trajectories at any finite time index remain Gaussian:

$$q(\mathbf{x}_t | \mathbf{x}_0) = \mathcal{N}(\mathbf{x}_t | \sqrt{\bar{\alpha}_t} \mathbf{x}_0; \Sigma_t), \quad \text{where} \quad \Sigma_t := (1 - \bar{\alpha}_t) \mathbf{I}. \quad (9)$$

In practice, the true data distribution $p_{\text{data}}(\mathbf{x})$ is often intractable, making the direct analytical derivation of the marginal $q(\mathbf{x}_t)$ equally infeasible. However, given a dataset $\mathcal{D} = \{\mathbf{x}^{(i)}\}_{i=1}^N$ with each $\mathbf{x}^{(i)} \in \mathbb{R}^d$, we could compute the empirical per-sample mean and variance as:

$$\mu^{(i)} = \frac{1}{d} \sum_{j=1}^d x_j^{(i)}, \quad v^{(i)} = \frac{1}{d} \sum_{j=1}^d (x_j^{(i)} - \mu^{(i)})^2. \quad (10)$$

We then aggregate these statistics across the dataset to obtain the *average per-sample variance* via $\hat{v} = \frac{1}{N} \sum_{i=1}^N v^{(i)}$. Unlike classical estimators of the global variance, which pool all data dimensions and samples into a single statistic, this approach estimates the expected per-sample first and second moments. This method has the following properties:

Proposition 1. *Under finite fourth-order moments, the average per-sample variance \hat{v} is an unbiased estimator of the expected per-sample variance.*

In contrast, while the average per-sample mean converges to the expected per-sample mean, its expectation can deviate significantly from the sample mean in datasets with heterogeneous or multi-modal structure (Lodhia et al., 2022). This discrepancy introduces instability and bias in generative processes that rely on the sample mean, for example, the posterior $q(\mathbf{x}_{t-1} | \mathbf{x}_t, \mathbf{x}_0)$ in Eq. 3. However, for many data modalities, it is both feasible and natural to preprocess data such that the mean is exactly zero (zero-mean), as illustrated in Sec. 2.2. Such centering preserves fundamental symmetries, such as translational invariance, without impairing generative modeling performance (Hoogeboom et al., 2022). In addition, it consistently enforces $\hat{\mu} = 0$, which avoids the bias in sample mean estimation.

Proposition 2. *For zero-mean invariant data, enforcing zero-centered mean does not incur any information loss in the model learning process.*

This property enables us to apply zero-mean preprocessing to various data modalities, such as point clouds, 3D molecular graphs, non-uniform one-hot encoded text, and more. The proof of Proposition 2 is provided in A. Throughout the remainder of this work, we assume that data has been preprocessed to have zero mean¹, and we therefore omit any explicit modeling of the data mean in our Gaussian approximations.

Under the variance-preserving (VP) forward process, the mean $\tilde{\mu}_t$ and variance \tilde{v}_t of \mathbf{x}_t evolve as:

$$\tilde{\mu}_t = \mathbf{0}, \quad \tilde{v}_t = 1 - \bar{\alpha}_t(1 - \hat{v}). \quad (11)$$

These statistics indicate that once the distribution of \mathbf{x}_t becomes sufficiently close to Gaussian (typically after a moderate number of noise steps), we can approximate the marginal distribution of \mathbf{x}_t as $\mathbf{x}_t \approx \mathcal{N}(\mathbf{0}, \tilde{v}_t \mathbf{I})$, as illustrated in Fig. 1. This Gaussian approximation underpins the trajectory shortening strategy introduced in the following sections.

3.2 EVALUATING GAUSSIANTITY: DATA IDENTITY AND DISTRIBUTIONAL SIMILARITY

While the preceding analysis suggests that \mathbf{x}_t may be approximated by a Gaussian with zero mean and analytically propagated variance, the validity of this approximation fundamentally depends on the specific data modality and the intrinsic structure of the data distribution $p_{\text{data}}(\mathbf{x})$, i.e., the Gaussianity of \mathbf{x}_t .

¹Some complex data distributions, such as natural images or videos, cannot be zero-meant without information loss. Because the mean component in the generated samples is agnostic to the model, making it impossible to reconstruct the original content from a zero-meant representation.

Data Identity and Dependency Decay. The timestep at which data loses its structural identity under progressive noise perturbation is closely tied to the characteristics of the underlying data manifold. As shown in Fig. 2, for modalities such as molecular data, where coordinate positions and discrete one-hot atom-type vectors are sparse and low-dimensional, injecting Gaussian noise rapidly dissolves the dependency structures and distinctive features of the original sample. In contrast, for complex data domains such as natural images, which are characterized by spatially correlated, high-dimensional structures and smooth local dependencies, the data retains its identity over significantly more noise steps.

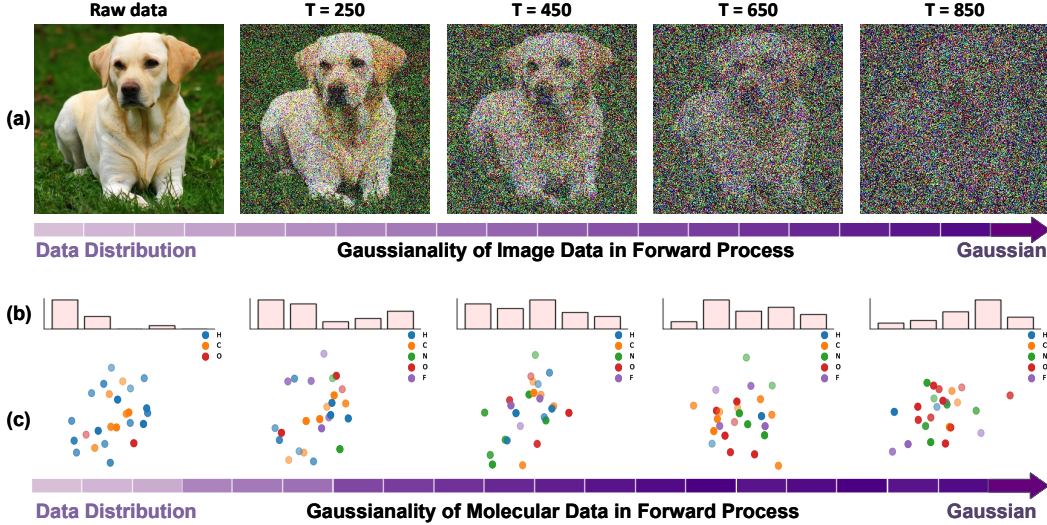


Figure 2: Comparisons of the forward noising process across different data modalities. (a) shows a continuous-valued image matrix, while (b) and (c) illustrate the distribution of one-hot vectors for atom types and Euclidean coordinates for atom positions, respectively, as used in molecular data. **The same noise schedule is applied across all modalities, with the number of steps T up to 1000.** Despite identical signal-to-noise ratios, image data retains recognizable structure for significantly more steps, whereas molecular representations attain sufficient Gaussianity much earlier.

To quantify the loss of data identity, we conceptualize it as the statistical dependency among the components of \mathbf{x}_t . As noise is progressively injected, the dependencies among dimensions diminish. Once the data consists of mutually independent entries, we consider it to have lost its identity. Let $\text{Dep}(\mathbf{x}_t)$ denote a functional measuring dependency strength, for example, mutual information or covariance norms. Under the variance-preserving (VP) schedule, the injected noise becomes increasingly dominant, leading to $\lim_{t \rightarrow T_{\text{ID}}} \text{Dep}(\mathbf{x}_t) \rightarrow 0$, where T_{ID} denotes the characteristic timestep at which data identity effectively vanishes. Beyond this point, the components of \mathbf{x}_t become approximately independent, justifying the approximation $\mathbf{x}_t \sim \mathcal{N}(\mathbf{0}, \text{Var}(\mathbf{x}_t) \mathbf{I})$.

Distributional Similarity. Beyond identity loss, we also quantitatively assess the Gaussianity of \mathbf{x}_t by measuring its distributional similarity to a theoretical Gaussian. Inspired by Massey Jr (1951), we compare the empirical cumulative distribution function (CDF) $F_{t,j}(x)$ of each dimension $\mathbf{x}_t^{(j)}$ to the Gaussian CDF $\Phi_{\sigma_t}(x)$ with matching variance σ_t^2 :

$$D_t = \frac{1}{d} \sum_{j=1}^d D_{t,j}, \quad \text{where} \quad D_{t,j} = \sup_x |F_{t,j}(x) - \Phi_{\sigma_t}(x)|. \quad (12)$$

A lower value of D_t indicates a higher degree of similarity to the reference Gaussian, thereby providing a quantitative justification for the Gaussian approximation of \mathbf{x}_t . As shown in Fig. 2, we find that molecular datasets exhibit rapid decay in D_t . It reflects the fast loss of data identity. In contrast, image data maintains larger D_t values over significantly more noise steps. From the dual perspective, data identity and distributional similarity, we form the foundation of our methodol-

ogy for determining when the Gaussian approximation of \mathbf{x}_t is valid. It also provides a principled criterion for selecting the characteristic step T^* at which the approximation can be safely applied.

Proposition 3. *Under a variance-preserving (VP) noise schedule, if at step T^* the variable \mathbf{x}_{T^*} exhibits high Gaussianity, i.e., it has lost its data identity and is well-approximated by a Gaussian distribution, then for any $s > T^*$, the Gaussianity of \mathbf{x}_s continues to increase, asymptotically converging to a pure Gaussian distribution as $s \rightarrow T$.*

The proof is provided in Appendix B. From a mathematical standpoint, \mathbf{x}_t remains non-Gaussian for all $t < T$ due to residual higher-order dependencies. However, once \mathbf{x}_{T^*} loses its structural identity, the subsequent latent states \mathbf{x}_t for $t > T^*$ contribute little meaningful information to the model. In fact, this phase of the trajectory introduces **redundancy**, not only incurring unnecessary computational cost but also potentially degrading generative performance:

- **Gradient Dilution:** Beyond T^* , additional noise injection results in training inputs that are nearly indistinguishable from pure Gaussian noise. This diminishes gradient magnitudes, impairing effective parameter updates.
- **Over-regularization:** Training on excessively noised inputs forces the model to extrapolate from unstructured representations to plausible outputs, which may result in suboptimal learning dynamics.
- **Transport Inefficiency:** In GPGMs, the reverse process must learn a transport map from an isotropic Gaussian to a structured target. When starting from \mathbf{x}_t that is already near-Gaussian, the remaining steps essentially map one Gaussian distribution to another. These transitions contribute marginally to likelihood maximization while incurring computational overhead and accumulating numerical integration error.

These factors indicate that once \mathbf{x}_{T^*} satisfies both sufficient Gaussianity and identity loss, continuing the forward (and consequently the reverse) process beyond T^* may be not only redundant, but also counterproductive. Accordingly, truncating or reparameterizing the generative process at T^* can improve both efficiency and fidelity in practice, as it eliminates ineffective training signals, reduces computational overhead, and avoids learning unnecessary transport dynamics between near-Gaussian distributions, which is empirically shown in Sec. 4.2.

4 EXPERIMENTS

In this section, we empirically evaluate our proposed method on standard molecular generative benchmarks. We describe the experimental setup, introduce evaluation metrics, and report quantitative results for both generation quality and efficiency. The details of the Gaussianity test settings are provided in Appendix C.

4.1 EXPERIMENT SETUP

Datasets. We conduct experiments on widely-used molecular datasets, QM9 (Ramakrishnan et al., 2014) and GEOM-Drugs (Axelrod & Gomez-Bombarelli, 2022). QM9 contains 130k small molecules with up to 29 atoms, while GEOM-Drugs comprises 450k drug-like molecules with an average of 44 and up to 181 atoms. The configuration of datasets follows Hooeboom et al. (2022) for regular generation and Xu et al. (2023) for latent-space generation, respectively.

Baselines. We conduct comparison experiments on several competitive baselines. G-Schnet (Gebauer et al., 2019) and Equivariant Normalizing Flows (ENF) (Garcia Satorras et al., 2021) employ autoregressive models for molecule generation. Equivariant Graph Diffusion Model (EDM) (Hooeboom et al., 2022), Geometric Latent Diffusion Model (GeoLDM) (Xu et al., 2023), and Equivariant Flow Matching model (EquiFM) (Song et al., 2023) are three representative GPGMs from different perspectives for molecule generation, including regular diffusion, latent diffusion, and flow-matching, respectively. Moreover, the invariant versions of EDM (GDM) and GeoLDM (GraphLDM) are also employed for comparison.

Metrics. We evaluate our method on standard molecular generation benchmarks using two broad classes of metrics: generation quality and efficiency. For generation quality, we report **validity** (the

proportion of chemically valid molecules according to standard valency checks), **uniqueness** (the proportion of distinct molecules among generated samples), **molecular stability** (the fraction of generated molecules satisfying correct valency constraints), and **atom stability** (the fraction of generated atoms satisfying correct valency constraints). Following prior work (Hong et al., 2025), these metrics are computed using RDKit-based validation and duplicate filtering over 10,000 generated samples. For efficiency, we record the average **sampling time (S-Time)** in GPU seconds per sample and total **training time (T-Time)** in GPU days, both measured on identical hardware before and after applying our Gaussian approximation strategy. Moreover, the **trajectory length (Steps)** T^* is also shown in the results. These metrics collectively quantify the fidelity, diversity, and practical computational benefits of our method.

4.2 MOLECULE GENERATION PERFORMANCE

Table 1: Quantitative results on the QM9 dataset. A higher number indicates better generation quality. Metrics are calculated using 10,000 samples generated from each model. Compared with previous methods, GA benefits all methods, achieving up to a 2.3% improvement in the Valid * Uniq metric, and significantly reduces the generation trajectory length by 40% without harming learning accuracy. All GA-compared baselines are tested using our implementation.

Model	Generation Performance				Efficiency		
	Atom Sta (%)	Mol Sta (%)	Valid (%)	Valid * Uniq (%)	S-Time (GPU sec.)	T-Time (GPU day)	Steps
Data	99.0	95.2	97.7	97.7	-	-	-
ENF	85.0	4.9	40.2	39.4	-	-	-
G-Schnet	95.7	68.1	85.5	80.3	-	-	-
GDM-AUG	97.6	71.6	90.4	89.5	0.52	-	1000
GraphLDM	97.2	70.5	83.6	82.7	-	-	1000
EDM	98.4	81.8	91.9	90.7	0.65	5.6	1000
EDM + GA	98.9	86.4	95.2	92.5	0.36	3.1	550
GeoLDM	98.9	89.8	94.0	91.9	0.64	11.7	1000
GeoLDM + GA	99.4	93.6	96.6	93.3	0.36	6.4	550
EquiFM	98.5	87.3	94.9	93.4	0.17	6.2	1000
EquiFM + GA	98.3	86.4	94.5	95.7	0.13	3.4	550

‘-’ denotes the invalid or not recorded setting in the original publication.

We evaluate the effectiveness of the proposed Gaussian Approximation (GA) across multiple molecular generative baselines on both the QM9 and GEOM-Drugs datasets. As shown in Tables 1 and 2, GA consistently improves generation quality while significantly reducing sampling cost. Crucially, our method shortens the diffusion trajectory, by up to 40%, without degrading the learning accuracy of the generative model. This is because GA does not alter the original noise schedule or variance scaling used during training; instead, it exploits the observation that molecular data loses its identity rapidly in the diffusion process, allowing training and sampling to begin from a later noise step without violating the underlying stochastic process. On the QM9 dataset, GA yields up to a 2.3% improvement in the *Valid * Uniq* metric, reflecting gains in both chemical correctness and diversity of the generated molecules.

Similar benefits are observed on the more challenging GEOM-Drugs dataset. However, we omit metrics such as uniqueness (which is consistently close to 100%) and molecule stability (which remains near 0%) due to their limited discriminative value across different methods on this dataset. Overall, GA consistently improves atom-level stability and reduces per-sample generation time across various baselines. These improvements are particularly noteworthy given that GA requires no changes to model architecture or parameters. Instead, it modifies only the generation trajectory length by leveraging the rapid identity decay characteristic of molecular structures. By analytically identifying a truncation to the Gaussian prior $\mathcal{N}(0, \tilde{v}_t)$ through zero-centering and dataset variance estimation, GA avoids redundant early steps in reverse process. This enables the model to focus on denoising stages where the molecular structure begins to emerge, leading to faster convergence without incurring additional transport cost or unnecessary noise inference from the skipped steps.

Table 2: Quantitative results on the GEOM dataset. A higher number indicates better generation quality. Metrics are calculated using 10,000 samples generated from each model. GA improves generation performance and provides better efficiency across models.

Model	Generation Performance		Efficiency	
	Atom Sta (%)	Valid (%)	S-Time (GPU sec.)	Steps
Data	86.5	99.9	–	–
GDM-AUG	77.7	91.8	–	1000
GraphLDM	76.2	97.2	–	1000
EDM	81.3	92.6	10.9	1000
EDM + GA	84.3	93.4	6.4	650
GeoLDM	84.4	99.3	10.2	1000
GeoLDM + GA	99.2	95.1	7.1	650

‘-’ denotes the invalid or not recorded setting in the original publication.

5 RELATED WORK

Probabilistic Generative Model (PGM). PGMs generate samples over data distributions by learning a transport process that maps simple prior distributions to complex data distributions through a sequence of structured transformations. Specifically, diffusion-based generative models simulate this sequential transformation via stochastic differential equations (SDEs), which have emerged as a powerful paradigm for multi-modal data synthesis (Croitoru et al., 2023; Kementzidis et al., 2025; Xu et al.). However, their iterative sampling (often requiring hundreds of steps) poses a significant speed bottleneck. A variety of techniques aim to accelerate diffusion sampling, such as progressive distillation (Salimans & Ho, 2022) and learned noising schedules (Williams et al., 2024). Nevertheless, the training process still typically requires hundreds of steps. Beyond diffusion models, Flow Matching offers a fresh perspective on acceleration. Flow Matching trains a continuous normalizing flow by regressing an optimal vector field along prescribed paths. Lipman et al. (2022) showed that using diffusion-style Gaussian paths in flow matching yields more robust training and faster ODE-based sampling. However, the nonlinear and high-curvature nature of learned transport fields makes it challenging to accurately approximate such trajectories with few discretization steps during training (Hassan et al., 2024; Eijkelboom et al., 2024).

Gaussian Approximation (GA). GA has long been a cornerstone in machine learning theory and practice. The Central Limit Theorem provides a classical justification: aggregates of many random factors tend toward a Gaussian distribution, which often explains why high-dimensional features or latent codes appear approximately normal (Hazra et al., 2021; Düker et al., 2024). Some researchers have explored the potential of the Gaussian approximation in generative modeling. For instance, Wang & Vastola observe that at high noise levels, the learned diffusion score can be well-approximated by a linear Gaussian model. Therefore, they could skip 15–30% of the sampling steps without degrading output fidelity. Such findings reinforce the idea that Gaussian assumptions can serve as an effective proxy for complex distributions in certain regimes, providing practical speedups without significant fidelity loss.

6 CONCLUSION AND FUTURE WORK

In this work, we introduced a principled framework for shortening generative trajectories in GPGMs. By leveraging zero-mean preprocessing and empirical variance estimation, we proposed an analytic Gaussian approximation that identifies a characteristic time step T^* at which data identity effectively vanishes and the forward process becomes distributionally Gaussian. This approximation enables the truncation of redundant noise steps without compromising the learning granularity of the model, thereby improving both sampling efficiency and training scalability. Furthermore, we showed that continuing trajectories beyond T^* might introduce barriers in model learning, e.g., diminishing gradient signals, over-regularization from unstructured inputs, and inefficient transport between near-Gaussian distributions. Each of them can hinder model performance. However, our method avoids these issues and yields consistent improvements in both quality and efficiency across multiple generative modeling benchmarks with different data modalities.

Future Work. Despite its empirical success, the current framework assumes that the data modality is *zero-mean invariant*, meaning that meaningful structure is preserved under empirical mean subtraction. While this assumption holds in many geometric and categorical domains, it is not valid for modalities like natural images or videos, where the absolute mean carries semantic information. Extending our methodology to such domains requires new techniques for identifying identity loss and Gaussianity without relying on zero-mean centering. A unified framework capable of accommodating both zero-mean invariant and non-invariant modalities would significantly enhance the generalization capability of Gaussian approximation strategies in probabilistic generative modeling.

REFERENCES

- Jacob Austin, Daniel D Johnson, Jonathan Ho, Daniel Tarlow, and Rianne Van Den Berg. Structured denoising diffusion models in discrete state-spaces. *Advances in neural information processing systems*, 34:17981–17993, 2021.
- Simon Axelrod and Rafael Gomez-Bombarelli. Geom, energy-annotated molecular conformations for property prediction and molecular generation. *Scientific Data*, 9(1):185, 2022.
- Andrew C Berry. The accuracy of the gaussian approximation to the sum of independent variates. *Transactions of the american mathematical society*, 49(1):122–136, 1941.
- Victor Chernozhukov, Denis Chetverikov, and Kengo Kato. Gaussian approximations and multiplier bootstrap for maxima of sums of high-dimensional random vectors. 2013.
- Florinel-Alin Croitoru, Vlad Hondru, Radu Tudor Ionescu, and Mubarak Shah. Diffusion models in vision: A survey. *IEEE Transactions on Pattern Analysis and Machine Intelligence*, 45(9):10850–10869, 2023.
- Hang Deng and Cun-Hui Zhang. Beyond gaussian approximation. *The Annals of Statistics*, 48(6):3643–3671, 2020.
- Marie-Christine Düker, Robert Lund, and Vladas Pipiras. High-dimensional latent gaussian count time series: Concentration results for autocovariances and applications. *Electronic Journal of Statistics*, 18(2):5484–5562, 2024.
- Floor Eijkelboom, Grigory Bartosh, Christian Andersson Naesseth, Max Welling, and Jan-Willem van de Meent. Variational flow matching for graph generation. *Advances in Neural Information Processing Systems*, 37:11735–11764, 2024.
- Victor Garcia Satorras, Emiel Hoogetboom, Fabian Fuchs, Ingmar Posner, and Max Welling. E (n) equivariant normalizing flows. *Advances in Neural Information Processing Systems*, 34:4181–4192, 2021.
- Niklas Gebauer, Michael Gastegger, and Kristof Schütt. Symmetry-adapted generation of 3d point sets for the targeted discovery of molecules. *Advances in neural information processing systems*, 32, 2019.
- Majdi Hassan, Nikhil Shenoy, Jungyoon Lee, Hannes Stärk, Stephan Thaler, and Dominique Beaini. Et-flow: Equivariant flow-matching for molecular conformer generation. *Advances in Neural Information Processing Systems*, 37:128798–128824, 2024.
- Arnab Hazra, Raphaël Huser, and Árni V Jóhannesson. Latent gaussian models for high-dimensional spatial extremes. *arXiv preprint arXiv:2110.02680*, 2021.
- Jonathan Ho, Ajay Jain, and Pieter Abbeel. Denoising diffusion probabilistic models. *arXiv preprint arXiv:2006.11239*, 2020.
- Haokai Hong, Wanyu Lin, and Kay Chen Tan. Accelerating 3d molecule generation via jointly geometric optimal transport. In *The Thirteenth International Conference on Learning Representations*, 2025.
- Emiel Hoogetboom, Victor Garcia Satorras, Clément Vignac, and Max Welling. Equivariant diffusion for molecule generation in 3d. In *International conference on machine learning*, pp. 8867–8887. PMLR, 2022.

- Tero Karras, Miika Aittala, Timo Aila, and Samuli Laine. Elucidating the design space of diffusion-based generative models. *Advances in neural information processing systems*, 35:26565–26577, 2022.
- Georgios Kementzidis, Erin Wong, John Nicholson, Ruichen Xu, and Yuefan Deng. An iterative framework for generative backmapping of coarse grained proteins. *arXiv preprint arXiv:2505.18082*, 2025.
- Bowen Li, Xiaojuan Qi, Thomas Lukasiewicz, and Philip Torr. Controllable text-to-image generation. *Advances in neural information processing systems*, 32, 2019.
- Yaron Lipman, Ricky TQ Chen, Heli Ben-Hamu, Maximilian Nickel, and Matt Le. Flow matching for generative modeling. *arXiv preprint arXiv:2210.02747*, 2022.
- Asad Lodhia, Keith Levin, and Elizaveta Levina. Matrix means and a novel high-dimensional shrinkage phenomenon. *Bernoulli*, 28(4):2578–2605, 2022.
- Cheng Lu, Yuhao Zhou, Fan Bao, Jianfei Chen, Chongxuan Li, and Jun Zhu. Dpm-solver: A fast ode solver for diffusion probabilistic model sampling in around 10 steps. *Advances in Neural Information Processing Systems*, 35:5775–5787, 2022.
- Frank J Massey Jr. The kolmogorov-smirnov test for goodness of fit. *Journal of the American statistical Association*, 46(253):68–78, 1951.
- Raghuathan Ramakrishnan, Pavlo O Dral, Matthias Rupp, and O Anatole Von Lilienfeld. Quantum chemistry structures and properties of 134 kilo molecules. *Scientific data*, 1(1):1–7, 2014.
- Tim Salimans and Jonathan Ho. Progressive distillation for fast sampling of diffusion models. *arXiv preprint arXiv:2202.00512*, 2022.
- Jiaming Song, Chenlin Meng, and Stefano Ermon. Denoising diffusion implicit models. *arXiv preprint arXiv:2010.02502*, 2020.
- Yuxuan Song, Jingjing Gong, Minkai Xu, Ziyao Cao, Yanyan Lan, Stefano Ermon, Hao Zhou, and Wei-Ying Ma. Equivariant flow matching with hybrid probability transport for 3d molecule generation. *Advances in Neural Information Processing Systems*, 36:549–568, 2023.
- Binxu Wang and John Vastola. The unreasonable effectiveness of gaussian score approximation for diffusion models and its applications. *Transactions on Machine Learning Research*.
- Christopher Williams, Andrew Campbell, Arnaud Doucet, and Saifuddin Syed. Score-optimal diffusion schedules. *arXiv preprint arXiv:2412.07877*, 2024.
- Minkai Xu, Lantao Yu, Yang Song, Chence Shi, Stefano Ermon, and Jian Tang. Geodiff: A geometric diffusion model for molecular conformation generation. In *International Conference on Learning Representations*.
- Minkai Xu, Alexander S Powers, Ron O Dror, Stefano Ermon, and Jure Leskovec. Geometric latent diffusion models for 3d molecule generation. In *International Conference on Machine Learning*, pp. 38592–38610. PMLR, 2023.
- Xuan Zhang, Limei Wang, Jacob Helwig, Youzhi Luo, Cong Fu, Yaochen Xie, Meng Liu, Yuchao Lin, Zhao Xu, Keqiang Yan, Keir Adams, Maurice Weiler, Xiner Li, Tianfan Fu, Yucheng Wang, Haiyang Yu, YuQing Xie, Xiang Fu, Alex Strasser, Shenglong Xu, Yi Liu, Yuanqi Du, Alexandra Saxton, Hongyi Ling, Hannah Lawrence, Hannes Stärk, Shurui Gui, Carl Edwards, Nicholas Gao, Adriana Ladera, Tailin Wu, Elyssa F. Hofgard, Aria Mansouri Tehrani, Rui Wang, Ameya Daigavane, Montgomery Bohde, Jerry Kurtin, Qian Huang, Tuong Phung, Minkai Xu, Chaitanya K. Joshi, Simon V. Mathis, Kamyar Azizzadenesheli, Ada Fang, Alán Aspuru-Guzik, Erik Bekkers, Michael Bronstein, Marinka Zitnik, Anima Anandkumar, Stefano Ermon, Pietro Liò, Rose Yu, Stephan Günnemann, Jure Leskovec, Heng Ji, Jimeng Sun, Regina Barzilay, Tommi Jaakkola, Connor W. Coley, Xiaoning Qian, Xiaofeng Qian, Tess Smidt, and Shuiwang Ji. Artificial intelligence for science in quantum, atomistic, and continuum systems. *arXiv preprint arXiv:2307.08423*, 2023.

Appendix

A PROOF FOR PROPOSITION 2

We aim to show that for data modalities satisfying zero-mean invariance, the operation of mean-centering preserves all structural information relevant to generative modeling. We mainly discuss the Euclidean and non-uniform one-hot cases, which are tested in our experiments.

Euclidean Data. Let $\{\mathbf{x}_i\}_{i=1}^n \subset \mathbb{R}^d$ denote a collection of n vectors (e.g., coordinates in a point cloud). Define the sample mean $\bar{\mathbf{x}} = \frac{1}{n} \sum_{i=1}^n \mathbf{x}_i$, and let $\tilde{\mathbf{x}}_i = \mathbf{x}_i - \bar{\mathbf{x}}$ be the centered representation. We claim that pairwise Euclidean distances are invariant under mean-centering:

$$\|\tilde{\mathbf{x}}_i - \tilde{\mathbf{x}}_j\|_2 = \|(\mathbf{x}_i - \bar{\mathbf{x}}) - (\mathbf{x}_j - \bar{\mathbf{x}})\|_2 = \|\mathbf{x}_i - \mathbf{x}_j\|_2. \quad (13)$$

Hence, all geometric properties that depend on inter-point distances, such as adjacency structures, bond lengths, or conformational shapes, are preserved exactly under centering. Consequently, zero-mean projection retains full information about the relational structure of the data.

Non-Uniform One-Hot Categorical Vectors. Let $h_i \in \{0, 1\}^d$ denote a one-hot encoded vector satisfying $\sum_{j=1}^d (h_i)_j = 1$, and let $\bar{h} = \frac{1}{n} \sum_{i=1}^n h_i$ be the sample mean across a batch of n such vectors. Define the centered vector $\tilde{h}_i = h_i - \bar{h}$. Note that each $\tilde{h}_i \in \mathbb{R}^d$ lies in a subspace orthogonal to the constant vector $\mathbf{1}_d$, since:

$$\sum_{j=1}^d (\tilde{h}_i)_j = \sum_{j=1}^d (h_i - \bar{h})_j = 1 - \sum_{j=1}^d \bar{h}_j = 0. \quad (14)$$

Moreover, the inner product between two centered vectors \tilde{h}_i and \tilde{h}_j satisfies:

$$\langle \tilde{h}_i, \tilde{h}_j \rangle = \langle h_i, h_j \rangle - \langle h_i, \bar{h} \rangle - \langle \bar{h}, h_j \rangle + \langle \bar{h}, \bar{h} \rangle, \quad (15)$$

from which it follows that pairwise centered dot products retain sufficient information to distinguish between original categorical identities once the category set is not degenerate (e.g., uniform). Since each one-hot vector h_i is uniquely defined by a single active index, subtracting the global mean \bar{h} merely induces a translation within the categorical simplex. The position of the maximal entry in \tilde{h}_i still identifies the active class as long as \bar{h} does not collapse distinct h_i vectors onto the same centered value. Therefore, for any non-uniform categorical data embedded via one-hot encoding, mean-centering preserves the identity of the active component up to an affine transformation of the ambient space. As a result, zero-mean preprocessing retains the categorical semantics necessary for generative modeling under Euclidean approximation schemes.

B PROOF OF PROPOSITION 3

We aim to show that under the variance-preserving (VP) diffusion process, once the variable x_t becomes sufficiently Gaussian, then for all future steps $s > t$, the distribution of x_s becomes progressively more Gaussian, asymptotically converging to a standard Gaussian as $s \rightarrow T$.

Setup. Let $\{x_t\}_{t=0}^T$ denote the latent trajectory generated by the forward diffusion process under a VP schedule. Fix a time $t \in [0, T]$, and consider a future timestep $s > t$. The marginal distribution of x_s conditional on x_t is given by:

$$x_s = \sqrt{\bar{\alpha}_{s|t}} x_t + \sqrt{1 - \bar{\alpha}_{s|t}} \epsilon, \quad \epsilon \sim \mathcal{N}(\mathbf{0}, \mathbf{I}), \quad (16)$$

where the rescaled signal-to-noise coefficient $\bar{\alpha}_{s|t} = \bar{\alpha}_s / \bar{\alpha}_t \in (0, 1)$ due to the monotonic decrease of the noise schedule.

Decay of Higher-Order Statistics. To analyze convergence toward Gaussianity, we examine the behavior of higher-order cumulants under this transformation. Recall that for any random vector x with cumulant tensor $C^{(k)}(x) \in \mathbb{R}^{d \times \dots \times d}$ of order $k \geq 3$, linear transformations attenuate cumulants multiplicatively. Specifically, if x is transformed as $x' = ax + b\epsilon$ for $a, b \in \mathbb{R}$ and $\epsilon \sim \mathcal{N}(0, \mathbf{I})$ independent of x , then:

$$C^{(k)}(x') = a^k C^{(k)}(x). \quad (17)$$

Applying this to our setting, we have:

$$C^{(k)}(x_s) = (\bar{\alpha}_{s|t})^{k/2} C^{(k)}(x_t), \quad \forall k \geq 3. \quad (18)$$

This shows that all non-Gaussian cumulants of x_s decay exponentially in k , since $\bar{\alpha}_{s|t} < 1$. In contrast, the first and second cumulants (mean and covariance) propagate linearly, and the added Gaussian noise ensures that the overall distribution remains strictly positive-definite in variance.

Convergence in Distribution. Because cumulants uniquely determine the distribution of a random variable (under standard moment conditions), the vanishing of all higher-order cumulants implies convergence to a Gaussian. Let $\mu_t = \mathbb{E}[x_t]$ and $\Sigma_t = \text{Cov}(x_t)$. Then, x_s converges in distribution to:

$$x_s \xrightarrow{d} \mathcal{N}(0, \Sigma_s), \quad \text{with} \quad \Sigma_s = \bar{\alpha}_{s|t} \Sigma_t + (1 - \bar{\alpha}_{s|t}) \mathbf{I}, \quad (19)$$

and $\Sigma_s \rightarrow \mathbf{I}$ as $s \rightarrow T$, given that $\bar{\alpha}_s \rightarrow 0$.

Total Variation Convergence. From Berry–Esseen-type bounds and functional central limit theorems, the decay of higher-order cumulants implies convergence in total variation distance between the distribution of x_s and the limiting Gaussian:

$$\text{TV}(x_s, \mathcal{N}(0, \Sigma_s)) \rightarrow 0 \quad \text{as} \quad s \rightarrow T. \quad (20)$$

Moreover, since Σ_s itself becomes increasingly isotropic, the full convergence is toward $\mathcal{N}(0, \mathbf{I})$. Therefore, once x_t has become sufficiently Gaussian (i.e., with negligible higher-order cumulants), all subsequent variables x_s ($s > t$) remain at least as Gaussian and approach the standard Gaussian asymptotically. This justifies truncating the generative trajectory at the earliest step T^* where x_{T^*} satisfies a chosen Gaussianity criterion. Beyond T^* , further forward steps only continue to contract the distribution toward the Gaussian prior without introducing new semantic information or structure, making them redundant from both modeling and computational perspectives.

C GAUSSIANTY TEST DETAILS

C.1 DEPENDENCY TEST

By treating x_t as a sample from an intractable noised data distribution, we estimate the empirical mutual information (MI) across both the sample-wise and feature-wise dimensions of the data tensor. MI quantifies the degree of statistical dependency between random variables by measuring the divergence between their joint distribution and the product of their marginals. For two random vectors X and Y , the mutual information is defined as:

$$I(X; Y) = \int \int p_{X,Y}(x, y) \log \frac{p_{X,Y}(x, y)}{p_X(x) p_Y(y)} dx dy, \quad (21)$$

where $p_{X,Y}(x, y)$ denotes the joint probability density, and $p_X(x), p_Y(y)$ are the marginal densities of X and Y , respectively.

Given a data matrix representation of x_t , we compute MI both row-wise and column-wise, that is, we estimate the dependency across dimensions (features) within each data point, and across data points for each dimension. Formally, let $\mathcal{X}_{\text{rows}}$ and $\mathcal{X}_{\text{cols}}$ denote the sets of row-wise and column-wise slices, respectively. Then, the empirical MI scores are given by:

$$\text{MI}_{\text{rows}} = \frac{1}{|\mathcal{X}_{\text{rows}}|} \sum_{x \in \mathcal{X}_{\text{rows}}} I(x), \quad \text{MI}_{\text{cols}} = \frac{1}{|\mathcal{X}_{\text{cols}}|} \sum_{x \in \mathcal{X}_{\text{cols}}} I(x), \quad (22)$$

where $I(x)$ denotes the estimated mutual information of the given vector x across its components. As t increases, these statistics decay toward zero, indicating diminishing dependency and the emergence of approximate independence in x_t .

C.2 DISTRIBUTIONAL SIMILARITY VIA KS-TEST

To evaluate whether the noised data x_t has become sufficiently similar to the Gaussian distribution $\mathcal{N}(0, \tilde{v}_t I)$, we perform statistical testing based on the Kolmogorov–Smirnov (KS) criterion. At each test timestep t , we apply the one-sample KS test dimension-wise to the components of x_t after zero-centering, treating each variable as an independent sample drawn from the empirical distribution. Specifically, for each dimension $j \in \{1, \dots, d\}$, we compute the empirical cumulative distribution function (CDF) $F_{t,j}(x)$ and compare it against the theoretical CDF $\Phi_{\tilde{v}_t}(x)$ of a univariate normal distribution with zero mean and variance \tilde{v}_t , derived analytically from the forward noise schedule. The test statistic is defined as:

$$D_{t,j} = \sup_x |F_{t,j}(x) - \Phi_{\tilde{v}_t}(x)|. \quad (23)$$

We reject the null hypothesis $H_0: "x_t^{(j)} \sim \mathcal{N}(0, \tilde{v}_t)"$ if $D_{t,j}$ exceeds the critical threshold at the 5% significance level. The overall test passes at timestep t if at least 95% of dimensions pass their individual KS tests. This formulation accounts for sample variability while ensuring a high-confidence Gaussianity assessment.

To determine whether the forward trajectory can be truncated at a given step T^* , we further leverage Proposition 3: once both x_t and $x_{t+\tau}$ (with $\tau = 25$ in our experiments) satisfy the Gaussianity criterion under the KS test, we assume that all subsequent $x_{t'}$ for $t' > t + \tau$ remain approximately Gaussian in distribution. Thus, we designate $T^* = t$ as the earliest time at which the KS test passes consistently across a sufficient range of future steps. This condition provides a principled and robust stopping rule for Gaussian approximation in the forward process.